Mon. Not. R. astr. Soc. (1986) **218,** 663–684

Dissipation of magnetic fields in very dense interstellar clouds – I. Formulation and conditions for efficient dissipation

Takenori Nakano and Toyoharu Umebayashi *Department of Physics, Kyoto University, Sakyo-ku, Kyoto 606, Japan*

Accepted 1985 August 21. Received 1985 August 19; in original form 1985 June 10

Summary. The drift velocity $\mathbf{v}_B$ of magnetic fields relative to the fluid is obtained by solving the motions of many kinds of charged particles. Any closed curve moving with $\mathbf{v}_B$ has a constant magnetic flux. This velocity contains the effects of both plasma drift and Joule dissipation. At the hydrogen density $n_H \lesssim 10^{11}\,\mathrm{cm}^{-3}$, v_B is at least 10 times smaller than the free-fall velocity u_f, and then field dissipation is inefficient. At $n_H \gtrsim 10^{12}\,\mathrm{cm}^{-3}$ and temperature $T < 10^3\,\mathrm{K}$ where thermal ionization is inefficient, however, v_B exceeds u_f unless the characteristic curvature radius of field lines is much greater than the characteristic length of the cloud. In such a situation, charged grains are more abundant than ions, and the field decays mainly through Joule dissipation. Thus the magnetic field is decoupled from the gas and only nearly current-free fields can exist in a part of the cloud with $n_H \gtrsim 10^{12}\,\mathrm{cm}^{-3}$ and $T < 10^3\,\mathrm{K}$.

1 Introduction

The magnetic force in the interstellar cloud is usually regarded as comparable with self-gravity. Therefore, it sometimes prevents the contraction of the cloud, and at least it reduces the rate of contraction to a considerable degree. The ratio of magnetic to gravitational force is proportional to the square of the magnetic-flux-to-mass ratio. A cloud of mass M and magnetic flux Φ can contract dynamically only when

$$\frac{\Phi}{M} < bG^{1/2} \tag{1}$$

is satisfied, where G is the gravitational constant and b is a quantity of the order of unity (Mestel 1965, 1966; Strittmatter 1966; Field 1970; Nakano 1981, 1984). Therefore, a cloud with a supercritical flux-to-mass ratio must become subcritical by losing some flux before it begins dynamic contraction.

Another problem of magnetic fields in star formation is in relation to the stellar magnetic fields. The surface magnetic fields of the Sun range from a few gauss in quiet regions to about 10^2 G in active regions. The fields in the sunspots amount to a few kilogauss. The magnetic stars with Ap

spectra have magnetic fields of typically a few hundred gauss. The range of measured fields is up to about 20 kG (Borra, Landstreet & Mestel 1982). Direct searches on non-Ap stars have brought about no really unambiguous evidence for the existence of sizeable coherent fields.

Even with the internal fields expected from the surface fields of magnetic stars, the magnetic force in a star is much weaker than the gravitational force, quite different from the interstellar cloud. This means that the magnetic-flux-to-mass ratio in the cloud is much greater than the ratio in the star. Nakano (1983a, 1984) showed that even the ratio in a subcritical cloud is 10^4–10^5 times the ratio in a typical magnetic star with a surface field of 1 kG and is at least 10^2 times the ratio in the most strongly magnetic stars. The mass of a cloud is nearly conserved because the accretion and evaporation of matter are negligible during the contraction. Therefore, a part of the cloud which will finally become a star must lose most of its initial magnetic flux in some stage of star formation.

As is well known, the magnetic fields in ordinary interstellar clouds are hardly dissipated by Joule heating even during the age of the Universe. Another possibility of dissipation is the drift of charged particles and magnetic fields in the sea of neutral gas particles as has been investigated by Mestel & Spitzer (1956) and by Cowling (1957). Since then, the magnetic flux loss by this process (plasma drift, also sometimes called ambipolar diffusion) has been investigated for various configurations of clouds [see review by Nakano (1984) and references therein]. Nakano (1979, 1982, 1983b) investigated the quasi-static contraction of magnetic clouds due to plasma drift and found that the contraction is highly non-homologous and the central core finally begins to contract dynamically. This core with stellar mass has a magnetic flux about 10^5 times the flux of a typical magnetic star even at the final stage of quasi-static contraction. With realistic densities of charged particles the time-scale of magnetic flux loss by plasma drift is more than 20 times the free-fall time of the cloud at the hydrogen density $n_H \lesssim 10^{10}\,\mathrm{cm}^{-3}$ (Nakano & Umebayashi 1980; Nakano 1981, 1984). Therefore, steep reduction of magnetic flux is impossible in clouds of these densities (Nakano 1984, 1985).

At $n_H \gtrsim 10^{10}\,\mathrm{cm}^{-3}$ the physical state of the clouds changes extensively:

(1) The ionization degree of the gas decreases as the density increases, and then the grains with charge $\pm e$ (e being the elementary electric charge) soon become the main charged particles (Umebayashi 1983; Nakano 1984).

(2) The ionization rate of gas by cosmic rays decreases exponentially as the column density of the cloud increases (Umebayashi & Nakano 1981), and the tendency (1) is further enhanced.

(3) Because of frequent collisions with neutral particles, even ions and electrons are hardly bound to the lines of magnetic force.

Spitzer (1963) noted that Joule dissipation becomes efficient when grains are the main charged particles. Nakano (1984) investigated the dissipation of magnetic fields in such situations for some configurations of clouds and found that the magnetic field decouples from the gas at $n_H \simeq 10^{12}\,\mathrm{cm}^{-3}$. He also investigated the magnetic flux brought into a newborn star and found that it is at most of the order of the flux of a magnetic star. In this series of papers we shall investigate these problems in greater detail.

In Section 2 we shall investigate the dissipation processes of magnetic fields and derive the drift velocity of magnetic fields relative to the neutrals which contains the effects of plasma drift and Joule dissipation. Comparing the drift velocity with the free-fall velocity, we shall investigate in Section 3 the dissipation of magnetic fields in the clouds of various configurations with density up to $10^{15}\,\mathrm{cm}^{-3}$ and clarify at what stage of contraction the magnetic field decouples from the gas. Some related problems are discussed in Section 4. The magnetic flux of a newborn star will be investigated in Paper II.

2 Dissipation processes of magnetic fields in slightly ionized gases

The effects of magnetic fields on the motion of electrons, ions and grains differ considerably because of the great differences in their masses. Moreover, their relative abundances vary greatly as the density increases from 10^4 to $10^{15}\,\mathrm{cm}^{-3}$. Hence the species playing the dominant role in coupling neutral particles with magnetic fields changes with the density. The dominant process of magnetic field dissipation also changes. Therefore, we must treat the problem in a rather general way. We derive the quantities fundamental in describing field dissipation and classify the dissipation processes.

2.1 MOTION OF PARTICLES ACROSS THE MAGNETIC FIELD

The interstellar cloud consists of many kinds of particle such as neutral molecules, electrons, various ions and dust grains of different electric charges. We shall regard neutral molecules as a single species although they are a mixture of hydrogen molecules and helium atoms. Because the ionization degree is extremely low, we can neglect the collisions between charged particles. We shall smooth the collisional interaction of charged particles with neutrals into a continuous force. Let m_α, n_α and $\mathbf{u}_\alpha$ be the mass, number density and velocity, respectively, in the inertial system of constituent α. Then the total momentum transferred to a charged constituent ν per unit volume per unit time in collisions with the neutral constituent n is given to a good approximation by

$$\mathbf{f}_{\nu\mathrm{n}}=\mu_{\nu\mathrm{n}}n_\nu n_\mathrm{n}\langle\sigma v\rangle_{\nu\mathrm{n}}(\mathbf{u}_\mathrm{n}-\mathbf{u}_\nu), \tag{2}$$

where $\mu_{\nu\mathrm{n}}$ $\{\equiv m_\nu m_\mathrm{n}/(m_\nu+m_\mathrm{n})\}$ is the reduced mass and $\langle\sigma v\rangle_{\nu\mathrm{n}}$ is the momentum-transfer rate coefficient for a particle ν colliding with neutrals averaged over the Maxwellian velocity distribution. The values of $\langle\sigma v\rangle_{\nu\mathrm{n}}$ for various charged particles are summarized in the Appendix.

The equation of motion for constituent ν other than neutrals is given by

$$\varrho_\nu\frac{d\mathbf{u}_\nu}{dt}=eq_\nu n_\nu\left(\mathbf{E}_0+\frac{1}{c}\,\mathbf{u}_\nu\times\mathbf{B}\right)-\nabla P_\nu+\varrho_\nu\mathbf{g}+\mathbf{f}_{\nu\mathrm{n}}, \tag{3}$$

where $d/dt\equiv\partial/\partial t+(\mathbf{u}_\nu\cdot\nabla)$ is the Lagrangian derivatives, ϱ_ν $(\equiv m_\nu n_\nu)$ and eq_ν are, respectively, the mass density and electric charge of constituent ν, $\mathbf{E}_0$ is the electric field in the inertial system, $\mathbf{B}$ the magnetic field, $\mathbf{g}$ the gravitational acceleration, c the light speed and $\boldsymbol{P}_\nu$ the stress tensor. In the simplest case where the distribution of the random velocity is isotropic, $\boldsymbol{P}_\nu$ reduces to a scalar pressure $P_\nu\boldsymbol{I}$, where $\boldsymbol{I}$ is the unit tensor. The equation of motion for a neutral constituent n is given by

$$\varrho_\mathrm{n}\frac{d\mathbf{u}_\mathrm{n}}{dt}=-\nabla\boldsymbol{P}_\mathrm{n}+\varrho_\mathrm{n}\mathbf{g}-\sum_\nu\mathbf{f}_{\nu\mathrm{n}}, \tag{4}$$

where ϱ_n $(\equiv m_\mathrm{n}n_\mathrm{n})$ and $\boldsymbol{P}_\mathrm{n}$ are the mass density and the stress tensor, respectively, and the summation Σ_ν extends over all charged species. In equations (3) and (4), we have neglected the effect of momentum transfer accompanying the transitions of charge states of particles. This effect is negligible as will be shown in Section 4.

The mass density and the velocity of the fluid as a whole are defined, respectively, by

$$\varrho=\varrho_\mathrm{n}+\sum_\nu\varrho_\nu, \tag{5}$$

$$\mathbf{u}=\frac{1}{\varrho}\left(\varrho_\mathrm{n}\mathbf{u}_\mathrm{n}+\sum_\nu\varrho_\nu\mathbf{u}_\nu\right). \tag{6}$$

From equations (3) and (4) the equation of motion of the fluid as a whole is easily reduced to

$$\varrho \frac{d\mathbf{u}}{dt}=\frac{1}{c}\mathbf{j}\times\mathbf{B}-\nabla P+\varrho\mathbf{g}, \tag{7}$$

where

$$\mathbf{j}=\sum_{\nu} eq_{\nu}n_{\nu}\mathbf{u}_{\nu} \tag{8}$$

is the electric current density, $\boldsymbol{P}$ is the stress tensor of the fluid as a whole and $d/dt\equiv\partial/\partial t+(\mathbf{u}\cdot\nabla)$. In deriving equation (7) the fluid is assumed to be electrically neutral, since the Debye shielding radius is negligible compared with the characteristic length of the interstellar clouds.

Because the ratio $\Sigma_{\nu}\varrho_{\nu}/\varrho_{\mathrm{n}}$ is very small in the interstellar cloud, the mass density ϱ and the velocity $\mathbf{u}$ of the fluid as a whole can be replaced by the mass density ϱ_{n} and the velocity $\mathbf{u}_{\mathrm{n}}$ of the neutrals, respectively. We introduce the velocity relative to the neutrals

$$\mathbf{v}_{\nu}=\mathbf{u}_{\nu}-\mathbf{u}_{\mathrm{n}}, \tag{9}$$

the electric field in the frame moving with the neutrals

$$\mathbf{E}=\mathbf{E}_0+\frac{1}{c}\mathbf{u}_{\mathrm{n}}\times\mathbf{B}, \tag{10}$$

and the viscous damping time of motion relative to the neutrals

$$\tau_{\nu}=\frac{\varrho_{\nu}}{\mu_{\nu\mathrm{n}}n_{\nu}n_{\mathrm{n}}\langle\sigma v\rangle_{\nu\mathrm{n}}}=\frac{m_{\mathrm{n}}+m_{\nu}}{m_{\mathrm{n}}}\frac{1}{n_{\mathrm{n}}\langle\sigma v\rangle_{\nu\mathrm{n}}}. \tag{11}$$

We also write

$$\mathbf{h}_{\alpha}\equiv\varrho_{\alpha}\mathbf{g}-\nabla P_{\alpha}-\varrho_{\alpha}\frac{d\mathbf{u}_{\alpha}}{dt}. \tag{12}$$

Then we have from equations (2)–(4)

$$eq_{\nu}n_{\nu}\left(\mathbf{E}+\frac{1}{c}\mathbf{v}_{\nu}\times\mathbf{B}\right)-\frac{\varrho_{\nu}}{\tau_{\nu}}\mathbf{v}_{\nu}+\mathbf{h}_{\nu}=0, \tag{13}$$

$$\sum_{\nu}\frac{\varrho_{\nu}}{\tau_{\nu}}\mathbf{v}_{\nu}+\mathbf{h}_{\mathrm{n}}=0 \tag{14}$$

for a charged particle ν and a neutral n, respectively. From the equation of motion for electrons [$\nu=e$ in equation (13)], we have

$$\mathbf{E}=-\frac{1}{c}\mathbf{v}_{\mathrm{e}}\times\mathbf{B}-\frac{m_{\mathrm{e}}}{e\tau_{\mathrm{e}}}\mathbf{v}_{\mathrm{e}}+\frac{1}{en_{\mathrm{e}}}\mathbf{h}_{\mathrm{e}}. \tag{15}$$

Substituting $\mathbf{E}$ in equation (15) into equation (13) for a charged constituent λ other than the electron, we have

$$\omega_{\lambda}\mathbf{v}_{\lambda}\times\mathbf{e}_{\mathrm{B}}-\frac{1}{\tau_{\lambda}}\mathbf{v}_{\lambda}+\frac{1}{\varrho_{\lambda}}\mathbf{h}_{\lambda}-\omega_{\lambda}\mathbf{v}_{\mathrm{e}}\times\mathbf{e}_{\mathrm{B}}-q_{\lambda}\frac{m_{\mathrm{e}}}{m_{\lambda}}\frac{1}{\tau_{\mathrm{e}}}\mathbf{v}_{\mathrm{e}}+q_{\lambda}\frac{1}{m_{\lambda}n_{\mathrm{e}}}\mathbf{h}_{\mathrm{e}}=0, \tag{16}$$

where

$$\omega_\lambda = q_\lambda \frac{eB}{m_\lambda c} \tag{17}$$

is the cyclotron frequency and $\mathbf{e}_B = \mathbf{B}/B$ is a unit vector in the direction of the magnetic field.

To solve these equations we introduce the local Cartesian coordinates (x, y, z) with the z axis along $\mathbf{B}$. In this section we consider only the motion in the (x, y) plane. Then all vectors except $\mathbf{e}_B$ in equations (13)–(16) are regarded as two dimensional in the (x, y) plane. We denote these two-dimensional vectors with a superscript $'$. In a way similar to that of Elmegreen (1979), equation (16) is solved as

$$\mathbf{v}'_\lambda = \mathbf{M}_\lambda \left(\frac{1}{\varrho_\lambda} \mathbf{h}'_\lambda - \omega_\lambda \mathbf{J}\mathbf{v}'_e - q_\lambda \frac{m_e}{m_\lambda} \frac{1}{\tau_e} \mathbf{v}'_e + q_\lambda \frac{1}{m_\lambda n_e} \mathbf{h}'_e \right), \tag{18}$$

where

$$\mathbf{M}_\lambda = \frac{1}{\Omega_\lambda^2} \left(\frac{1}{\tau_\lambda} \mathbf{I} + \omega_\lambda \mathbf{J} \right), \tag{19}$$

$$\Omega_\lambda^2 = \frac{1}{\tau_\lambda^2} + \omega_\lambda^2, \tag{20}$$

$$\mathbf{I} = \begin{pmatrix} 1 & 0 \\ 0 & 1 \end{pmatrix}, \qquad \mathbf{J} = \begin{pmatrix} 0 & 1 \\ -1 & 0 \end{pmatrix}. \tag{21}$$

Substituting equation (18) into the two-dimensional equation (14) and using the two-dimensional equation of motion (7) of the fluid as a whole, we have (see also Nakano 1984)

$$\left(A_1 + \frac{A_2}{\tau_e \omega_e} \right) \mathbf{v}'_e - \left(A_2 - \frac{A_1}{\tau_e \omega_e} \right) \mathbf{J}\mathbf{v}'_e = \frac{1}{c} (\mathbf{j} \times \mathbf{B})' + \sum_\nu \left(\frac{\omega_\nu}{\Omega_\nu} \right)^2 \mathbf{h}'_\nu - \sum_\nu \frac{\omega_\nu}{\tau_\nu \Omega_\nu^2} \mathbf{J}\mathbf{h}'_\nu + \frac{A_2}{\varrho_e \omega_e} \mathbf{h}'_e + \frac{A_1}{\varrho_e \omega_e} \mathbf{J}\mathbf{h}'_e, \tag{22}$$

where

$$A_1 = \sum_\nu \frac{\varrho_\nu \omega_\nu^2}{\tau_\nu \Omega_\nu^2}, \tag{23}$$

$$A_2 = \sum_\nu \frac{\varrho_\nu \omega_\nu}{\tau_\nu^2 \Omega_\nu^2}. \tag{24}$$

However, by using equation (7) the magnetic force is written as

$$\frac{1}{c} \mathbf{j} \times \mathbf{B} = \varrho \frac{d\mathbf{u}}{dt} + \nabla P - \varrho \mathbf{g}. \tag{25}$$

In a much simpler system in which ions and electrons are the only charged particles, the gravities, stress tensors and inertias of ions and electrons are easily found to be negligible (Mestel & Spitzer 1956). In our case, however, some further consideration is necessary.

Since $(\omega_\nu/\Omega_\nu)^2$ and $|\omega_\nu/\tau_\nu \Omega_\nu^2|$ are always smaller than unity, the terms in equation (22) involving Σ_ν are at most comparable with $\Sigma_\nu |\mathbf{h}'_\nu|$. Because $\varrho_\nu \ll \varrho$ in the slightly ionized gas, the

gravity and the force due to the stress tensor in $\mathbf{h}_\nu'$ given by equation (12) are negligible compared with the corresponding terms in equation (25). Because the viscous damping times τ_ν are much smaller than a typical time-scale of the cloud as will be shown in Section 4, $d\mathbf{u}_\nu/dt$ cannot deviate much from $d\mathbf{u}/dt$. Therefore, the inertia term in $\mathbf{h}_\nu'$ can also be neglected compared with that in equation (25). Since $|A_2/\varrho_e\omega_e| = |\Sigma_\nu q_\nu n_\nu/\tau_\nu^2\Omega_\nu^2|/n_e$ and $\tau_\nu^2\Omega_\nu^2 > 1$, this ratio is at most unity when ions and electrons are the main charged particles. When grains are the main charges, this ratio is less than n_i/n_e which is at most about 230 (Umebayashi 1983; Nakano 1984), where the subscript i refers to ions. An upper bound of $A_1/|\varrho_e\omega_e| = \Sigma_\nu q_\nu n_\nu \tau_\nu \omega_\nu/\tau_\nu^2\Omega_\nu^2/n_e$ is unity when ions and electrons are the main charges. When grains are the main charges, this ratio is at most 10^3 for the magnetic field anticipated in dense clouds [e.g. Nakano's (1984) equation (7.10)] and for the densities of electrons and charged grains shown in Fig. 3. Because these upper bounds are much less than ϱ/ϱ_e, each term of $\mathbf{h}_e'$ in equation (22) can also be neglected compared with the corresponding term in equation (25).

Apart from the term $(1/c)(\mathbf{j}\times\mathbf{B})'$, the greatest contribution to the right-hand side of equation (22) would come from the gravity on grains because of their highest fractional mass $\varrho_g/\varrho \simeq 10^{-2}$, where the subscript g refers to grains. Therefore, as long as $(1/c)(\mathbf{j}\times\mathbf{B})$ is greater than $10^{-2}\varrho\mathbf{g}$, the gravity term on grains can be neglected. As for charged grains ν of any charge we find $|\tau_\nu\omega_\nu| < 1$ at $n_H \gtrsim 10^5\ \mathrm{cm}^{-3}$ even for such a strong field as $(1/c)(\mathbf{j}\times\mathbf{B}) \simeq \varrho\mathbf{g}$ (see for example Fig. 1). Therefore, even when $(1/c)(\mathbf{j}\times\mathbf{B})$ is considerably smaller than $10^{-2}\varrho\mathbf{g}$, the gravity term on grains can be neglected because $(\omega_\nu/\Omega_\nu)^2 \propto B^2 \propto (1/c)|\mathbf{j}\times\mathbf{B}|$ for grains. Thus we have

$$\left(A_1+\frac{A_2}{\tau_e\omega_e}\right)\mathbf{v}_e'-\left(A_2-\frac{A_1}{\tau_e\omega_e}\right)\mathbf{J}\mathbf{v}_e'=\frac{1}{c}(\mathbf{j}\times\mathbf{B})'. \tag{26}$$

Taking the local x axis in the direction of $\mathbf{j}\times\mathbf{B}$, we can solve equation (26) as

$$v_{ex}=\left(\frac{\omega_e}{\Omega_e}\right)^2\frac{1}{A}\left(A_1+\frac{A_2}{\tau_e\omega_e}\right)\frac{1}{c}(\mathbf{j}\times\mathbf{B})_x, \tag{27}$$

$$v_{ey}=\left(\frac{\omega_e}{\Omega_e}\right)^2\frac{1}{A}\left(\frac{A_1}{\tau_e\omega_e}-A_2\right)\frac{1}{c}(\mathbf{j}\times\mathbf{B})_x, \tag{28}$$

where

$$A=A_1^2+A_2^2$$

$$=\sum_{\varkappa,\nu}\frac{\varrho_\varkappa\omega_\varkappa}{\tau_\varkappa^2\Omega_\varkappa^2}\frac{\varrho_\nu\omega_\nu}{\tau_\nu^2\Omega_\nu^2}(\tau_\varkappa\omega_\varkappa\tau_\nu\omega_\nu+1). \tag{29}$$

Equation (22) holds even when the subscript e is replaced by λ, an arbitrary charged constituent. In a similar way as above, the terms with $\mathbf{h}_\lambda$ and $\mathbf{h}_\nu$ are found to be negligible, and we obtain

$$v_{\lambda x}=\left(\frac{\omega_\lambda}{\Omega_\lambda}\right)^2\frac{1}{A}\left(A_1+\frac{A_2}{\tau_\lambda\omega_\lambda}\right)\frac{1}{c}(\mathbf{j}\times\mathbf{B})_x, \tag{30}$$

$$v_{\lambda y}=\left(\frac{\omega_\lambda}{\Omega_\lambda}\right)^2\frac{1}{A}\left(\frac{A_1}{\tau_\lambda\omega_\lambda}-A_2\right)\frac{1}{c}(\mathbf{j}\times\mathbf{B})_x. \tag{31}$$

These equations are also obtained by substituting equations (27) and (28) into equation (18) and by neglecting the terms in $\mathbf{h}_\lambda$ and $\mathbf{h}_e$.

By neglecting the $\mathbf{h}_e$ term in equation (15) the two-dimensional electric field is expressed as

$$\mathbf{E}'=-\frac{1}{c}(\mathbf{v}_B\times\mathbf{B})', \tag{32}$$

where

$$\mathbf{v}'_B=\mathbf{v}'_e+\frac{1}{\tau_e\omega_e}\mathbf{J}\mathbf{v}'_e. \tag{33}$$

Let us consider an arbitrary closed curve C in the fluid. The magnetic flux Φ through this curve changes with time as

$$\frac{d\Phi}{dt}=\int_S\frac{\partial\mathbf{B}}{\partial t}\cdot d\mathbf{S}+\oint_C\mathbf{B}\cdot(\mathbf{u}\times d\boldsymbol{\tau}), \tag{34}$$

where S is a surface encircled by C and $\mathbf{u}$ is the velocity of the curve. Using the relation

$$\frac{\partial\mathbf{B}}{\partial t}=-c\nabla\times\mathbf{E}_0 \tag{35}$$

and Stokes' theorem, we have

$$\frac{d\Phi}{dt}=-c\oint_C\left(\mathbf{E}_0+\frac{1}{c}\mathbf{u}\times\mathbf{B}\right)\cdot d\boldsymbol{\tau}. \tag{36}$$

From equations (10) and (36) we find that Φ is constant when the curve C moves with the relative velocity $\mathbf{u}-\mathbf{u}_n$ equal to $\mathbf{v}'_B$ given by equation (33). Thus we can see that the magnetic field moves with the relative velocity $\mathbf{v}'_B$. Substituting equations (27) and (28) into equation (33), we have

$$v_{Bx}=\frac{A_1}{A}\frac{1}{c}(\mathbf{j}\times\mathbf{B})_x, \tag{37}$$

$$v_{By}=-\frac{A_2}{A}\frac{1}{c}(\mathbf{j}\times\mathbf{B})_x. \tag{38}$$

It should be noticed that both components of the drift velocity $\mathbf{v}'_B$ are proportional to the strength of the magnetic force. A similar picture on the behaviour of magnetic fields has been obtained by Sweet (1950) for a much simpler system.

Apart from the effect of induction accompanying the fluid motion $\mathbf{u}_n$, the density of magnetic energy changes with the rate of work $\mathbf{j}\cdot\mathbf{E}$. Because $j_x=0$ in our local Cartesian coordinates, the change in magnetic energy is determined only by the y component of $\mathbf{E}$, and then by the x component of $\mathbf{v}_B$. Equation (37) for v_{Bx} has also been obtained by Nakano (1984) for axisymmetric clouds.

2.2 DISSIPATION PROCESSES OF MAGNETIC FIELDS

We shall express the electric field in terms of other physical quantities so as to interpret clearly the dissipation processes of the magnetic field.

Because $\mathbf{h}_\nu$ is negligible, the z component of equation (13) is solved for $v_{\nu z}$ as

$$v_{\nu z}=\frac{eq_\nu\tau_\nu}{m_\nu}E_z. \tag{39}$$

From equations (8), (9) and (39) and the electrical neutrality, we have

$$E_z=\frac{j_z}{\sigma_c}. \tag{40}$$

where σ_c is the electrical conductivity along the magnetic field and is given as a sum of the contributions from all kinds of charged particles:

$$\sigma_c=\Sigma_\nu \sigma_c(\nu). \tag{41}$$

$$\sigma_c(\nu)=\frac{(eq_\nu)^2\tau_\nu n_\nu}{m_\nu}. \tag{42}$$

From equations (32), (37), (38), (41) and (42), the other components of **E** are written as

$$E_x=\beta(\mathbf{j}\times\mathbf{B})_x, \tag{43}$$

$$E_y=\frac{j_y}{\sigma_c}-\xi\{(\mathbf{j}\times\mathbf{B})\times\mathbf{B}\}_y, \tag{44}$$

where

$$\beta=\frac{B}{c^2}\frac{A_2}{A}, \tag{45}$$

$$\xi=\frac{1}{c^2}\frac{A_1}{A}-\frac{1}{B^2\sigma_c}$$

$$=\frac{1}{B^2\sigma_c A}\sum_{\varkappa,\nu}\frac{\varrho_\varkappa\omega_\varkappa}{\tau_\varkappa^2\Omega_\varkappa^2}\frac{\varrho_\nu\omega_\nu}{\tau_\nu^2\Omega_\nu^2}\{\tau_\varkappa\omega_\varkappa(\tau_\nu\omega_\nu)^3-1\}. \tag{46}$$

In our local Cartesian coordinates with the x axis along $\mathbf{j}\times\mathbf{B}$ and the z axis along **B**, $j_x=0$ and the vector $(\mathbf{j}\times\mathbf{B})\times\mathbf{B}$ is parallel to the y axis. Therefore, substituting equations (40), (43) and (44) into equation (10), we obtain for the electric field in the inertial system

$$\mathbf{E}_0=-\frac{1}{c}\mathbf{u}_n\times\mathbf{B}+\frac{1}{\sigma_c}\mathbf{j}+\beta\mathbf{j}\times\mathbf{B}-\xi(\mathbf{j}\times\mathbf{B})\times\mathbf{B}. \tag{47}$$

When the displacement current can be ignored, the volume integral to infinity of $\mathbf{j}\cdot\mathbf{E}_0$ is equal to the rate of decrease in the total magnetic energy. Thus the rate of decrease in the magnetic energy density $B^2/8\pi$ is linked with the rate of working per unit volume $\mathbf{j}\cdot\mathbf{E}_0$ of the electromagnetic forces on the particles. The first term on the right-hand side of equation (47) yields the rate of working $(1/c)(\mathbf{j}\times\mathbf{B})\cdot\mathbf{u}_n$ of the Lorentz body force on the bulk fluid motion. The so-called Joule dissipation is induced by the second term. The third term perpendicular to **j** does not contribute to the dissipation. The fourth term causes dissipation due to plasma drift, which is more important than Joule dissipation when the magnetic field is sufficiently strong. Thus the drift velocity $\mathbf{v}_B$ of the magnetic field given by equations (37) and (38) contains the effects of both Joule dissipation and plasma drift. When the charged particles other than electrons and ions are negligible, equation (47) reduces to the equation obtained by Cowling (1957) [see also equation (21) in the forthcoming Paper II].

The relative rate of plasma drift and Joule dissipation is given by the ratio of the fourth to the

second term on the right-hand side of equation (47):

$$D \equiv B^2 \xi \sigma_c$$

$$= \frac{1}{A} \sum_{\varkappa,\nu} \frac{\varrho_\varkappa \omega_\varkappa}{\tau_\varkappa^2 \Omega_\varkappa^2} \frac{\varrho_\nu \omega_\nu}{\tau_\nu^2 \Omega_\nu^2} \{\tau_\varkappa \omega_\varkappa (\tau_\nu \omega_\nu)^3 - 1\}. \tag{48}$$

When charged particles other than ions and electrons are negligible, equation (48) reduces to

$$D \simeq -\tau_e \omega_e \tau_i \omega_i. \tag{49}$$

Therefore, as long as $|\tau_e \omega_e \tau_i \omega_i| > 1$ and $n_i \simeq n_e \gg n_g$, the magnetic field is mainly dissipated by the plasma drift. When the effects of charged particles other than grains of charge $\pm e$ are negligible, we have

$$D \simeq -\tau_+ \omega_+ \tau_- \omega_-, \tag{50}$$

where the subscripts $\pm$ refer to grains of charge $\pm e$. When the effects of ions and electrons are negligible, we have $|\tau_+ \omega_+ \tau_- \omega_-| \ll 1$ for the field strength anticipated in the cloud, and then the field decays mainly through Joule dissipation.

3 Numerical results

Using the results obtained in Section 2, we investigate the dissipation of magnetic fields in some configurations of dense interstellar clouds and clarify in what situations the magnetic field decouples from the contracting gas.

From equations (10) and (32), we have

$$\mathbf{E}_0' = -\frac{1}{c} \{(\mathbf{u}_n + \mathbf{v}_B) \times \mathbf{B}\}' \tag{51}$$

in the local (x, y) plane perpendicular to the magnetic field. The $\mathbf{u}_n \times \mathbf{B}$ term in this equation induces the time variation of magnetic fields due to fluid motion, and the $\mathbf{v}_B \times \mathbf{B}$ term brings about the decay of fields due to plasma drift and Joule dissipation. Because $j_x = 0$ in our local coordinate system, the dissipation of magnetic fields is determined by v_{Bx}. When v_{Bx} is much smaller than u_n, the magnetic field is nearly frozen to the gas. In contrast, when v_{Bx} is greater than u_n, the field is nearly decoupled from the gas. Therefore, the degree of coupling of field and gas is inferred from the ratio v_{Bx}/u_n.

Throughout this series of papers we adopt the usual interstellar abundances of elements: the fractional masses of hydrogen and helium are $X = 0.73$ and $Y = 0.25$, respectively, and the abundances and depletion of heavy elements are the same as in the paper by Umebayashi & Nakano (1980). Then we find that the mean molecular weight μ of the gas equals 2.34. The gas is ionized by cosmic rays and radioactive elements, and ions and electrons annihilate through radiative, dissociative and grain-surface recombinations. We determine the equilibrium densities of charged particles with the models constructed by Umebayashi & Nakano (1980) and Umebayashi (1983) with the following modifications:

(1) The sticking probability of electrons on dust grains, S_e, is set equal to unity, regardless of the gas temperature.

(2) The desorption of charged particles from grains is neglected even at high temperatures.

(3) Since grains of high electric charge are scarce in dense clouds, we only include grains of charge $\pm e$ and 0 (neutral) in our reaction scheme.

As will be confirmed later, the abundances of charged particles are affected little by these modifications (see Fig. 3). We assume that all grains have the same size and properties and that the total missing amount of rocky and metallic materials in the gas phase relative to the solar abundances is all locked up in grains. Neglect of icy material affects the following results little (see also Section 4). Taking the grain radius a equal to 1.0×10^{-5} cm and the internal density of grains ϱ_s to be $3\,\mathrm{g\,cm^{-3}}$, we have the relative number density n_g/n_H of grains approximately equal to 10^{-12}. Since the heavy metal ions are the major ions (Umebayashi & Nakano 1980; Umebayashi 1983), it is sufficient in our problem to consider electrons, heavy metal ions and grains of charge $\pm e$ as charged particles.

3.1 THE MEAN DRIFT VELOCITY

Let us consider an oblate spheroidal cloud of mass M, semimajor axis R across the magnetic field and semiminor axis Z along the field. The mean density ϱ and the mean column density s along the field are given by

$$\varrho\simeq\frac{3M}{4\pi R^2Z}, \tag{52}$$

$$s\simeq\frac{M}{\pi R^2}. \tag{53}$$

Because we are interested in the clouds of mean hydrogen number density n_H up to $10^{15}\,\mathrm{cm^{-3}}$, we must take account of the increase in the gas temperature and the decrease in the ionization rate by cosmic rays in calculating the densities of charged particles. The temperature T as a function of n_H is determined as follows: (1) from evolutionary paths of clouds given by Hattori, Nakano & Hayashi (1969) in the transparent and early opaque stages when the clouds contract nearly isothermally; (2) from paths of the cloud cores obtained by Nakano, Ohyama & Hayashi (1968) in the opaque stages when the clouds contract nearly adiabatically. The ionization rate of a hydrogen molecule at a depth χ (in $\mathrm{g\,cm^{-2}}$) from the cloud surface is given by

$$\zeta(\chi)=\zeta_0\exp\left(\frac{-\chi}{\lambda}\right)+\zeta_R, \tag{54}$$

where $\lambda\simeq96\,\mathrm{g\,cm^{-2}}$ is the attenuation length of the ionization rate, $\zeta_0\simeq1\times10^{-17}\,\mathrm{s^{-1}}$ is the ionization rate by cosmic rays in the interstellar space and $\zeta_R\simeq6.9\times10^{-23}\,\mathrm{s^{-1}}$ is the rate by radioactive elements in the cloud (Umebayashi & Nakano 1981). In this section we use the ionization rate at a depth $\chi=s/2$.

In calculating the drift velocity v_{Bx} according to equation (37) we replace $(1/c)(\mathbf{j}\times\mathbf{B})_x$ with the mean magnetic force $B^2/4\pi Z$, where B is the mean field strength in the cloud. The cloud is nearly in equilibrium when $B^2/4\pi Z\simeq\varrho GM/R^2$ holds, i.e. B is equal to the critical field:

$$B_{cr}\simeq2\pi G^{1/2}s. \tag{55}$$

Because we are mainly interested in the quasi-static and dynamic contradictions of clouds, we shall consider the cases of $B\lesssim B_{cr}$ which is equivalent to equation (1). As the typical velocity u_n in the cloud we take the free-fall velocity in the r direction:

$$u_f=\left(\frac{2GM}{R}\right)^{1/2}. \tag{56}$$

Although a magnetic cloud is usually non-spherical, we consider in the first place a spherical

cloud ($Z \simeq R$) as a limiting case. The results for a cloud of mass $M=1\,M_\odot$ are shown in Figs 1–3. The solid curves in Fig. 1 show the contours of v_{Bx}/u_f=constant on the (n_H, B) plane. The dot-dashed line shows the critical field B_{cr} given by equation (55). As long as the magnetic field is frozen to the gas, a spherical cloud contracts parallel to this line. The condition $|\tau_\nu \omega_\nu|=1$ holds for a charged particle ν at the field strength

$$B_\nu = \frac{c\mu_{\nu n} n_n \langle \sigma v \rangle_{\nu n}}{e|q_\nu|}. \tag{57}$$

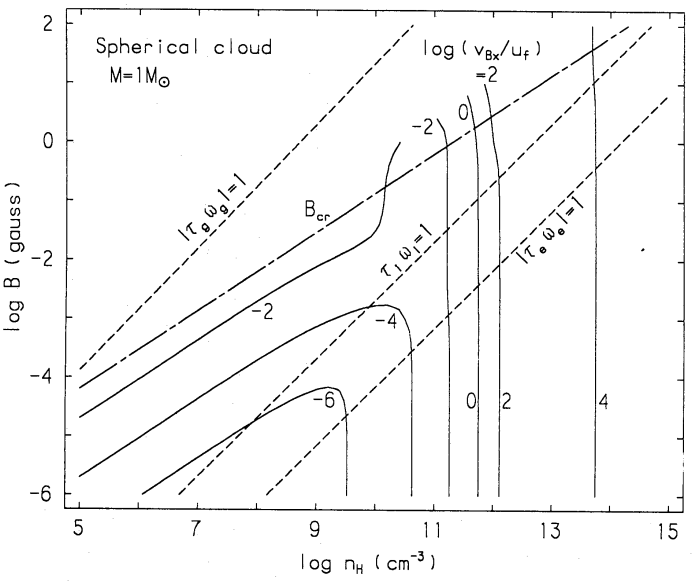

Figure 1. The drift velocity v_{Bx} of the magnetic field as a function of the mean density n_H and the mean field strength B for a spherical cloud of $1\,M_\odot$. The solid curves represent the contours of constant v_{Bx}/u_f and are labelled by the values of $\log(v_{Bx}/u_f)$ where u_f is the free-fall velocity. The dot-dashed line represents the critical field B_{cr} for contraction given by equation (55). The dashed lines represent the field strength for the state $|\tau_\nu \omega_\nu|=1$ given by equation (57) for electrons, ions and grains of charge $\pm e$.

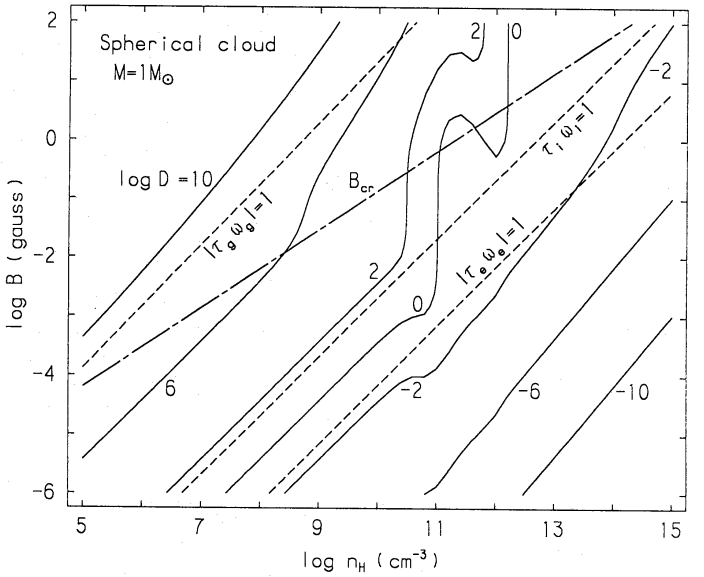

Figure 2. The ratio of the effects of plasma drift and Joule dissipation D defined by equation (48) as a function of the mean density n_H and the mean field strength B for a spherical cloud of $1\,M_\odot$. The solid curves represent the contours of constant D and are labelled by the values of $\log D$. The critical field B_{cr} and the states $|\tau_\nu \omega_\nu|=1$ are shown by the dot-dashed and the dashed lines, respectively.

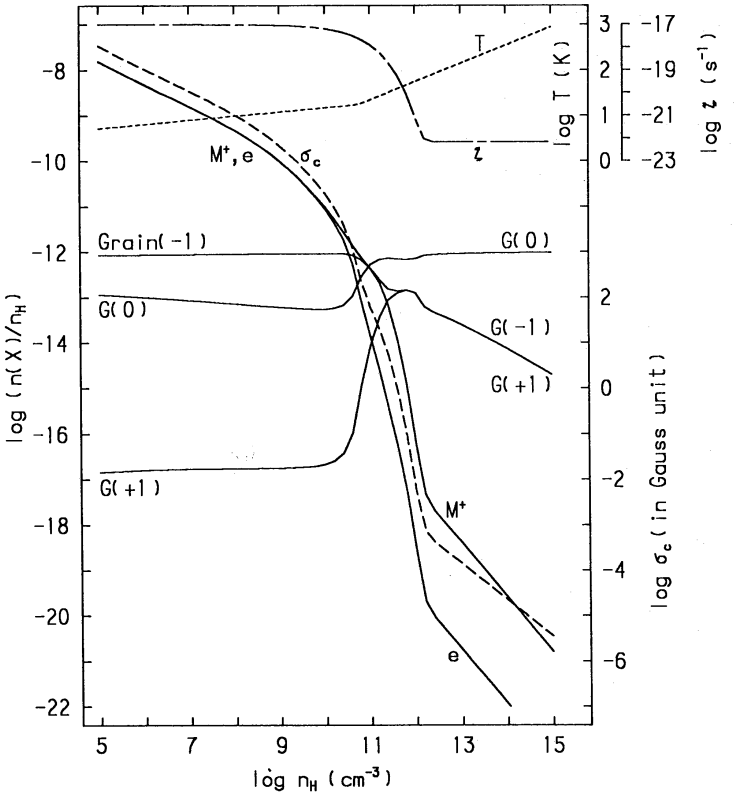

Figure 3. Relative abundances $n(\mathrm{X})/n_{\mathrm{H}}$ of some representative charged particles as functions of the mean density n_{H} for a spherical cloud of 1 $M_{\odot}$. The electric conductivity σ_{c} given by equation (41) is also shown by the dashed curve. The dashed curve and the dot-dashed curve in the upper part of the figure represent the gas temperature T and the ionization rate $\zeta(\chi)$ evaluated by equation (54), respectively.

The field strengths B_{ν} for electrons, heavy metal ions and grains of charge $\pm e$ are also shown by the dashed lines. When the magnetic field is stronger than B_{ν}, the particle ν is nearly frozen to the magnetic field.

At densities $n_{\mathrm{H}} \lesssim 10^{11}\,\mathrm{cm}^{-3}$, v_{Bx} is always much smaller than u_{f}. Because v_{Bx} is proportional to the magnetic force, v_{Bx} increases as B increases. However, v_{Bx} is at least 20 times smaller than u_{f} as long as $B \lesssim B_{\mathrm{cr}}$. This means that the dissipation of magnetic fields is inefficient at such densities. These results agree with those of Nakano & Umebayashi (1980). They found that the time-scale $t_{\mathrm{B}} \simeq R/v_{\mathrm{ex}}$ of magnetic flux loss for a spherical cloud of 1 $M_{\odot}$ with $B \simeq B_{\mathrm{cr}}$ is about 20 times greater than the free-fall time $t_{\mathrm{f}}=(3\pi/32G\varrho)^{1/2}$. Because $|\tau_{\mathrm{e}}\omega_{\mathrm{e}}| \gg 1$ in such a situation, we have $v_{\mathrm{ex}} \simeq v_{Bx}$ from equations (27) and (37).

At $n_{\mathrm{H}} \gtrsim 10^{11}\,\mathrm{cm}^{-3}$, v_{Bx} begins to increase rapidly with density, and it becomes equal to u_{f} at $n_{\mathrm{H}} \simeq 5\times10^{11}\,\mathrm{cm}^{-3}$. Above this density, v_{Bx} greatly exceeds u_{f}. It should be noticed that this behaviour of v_{Bx} is nearly independent of the field strength B. Thus we can conclude that the magnetic field is decoupled from the gas at $n_{\mathrm{H}} \gtrsim 5\times10^{11}\,\mathrm{cm}^{-3}$. These results agree well with those obtained by Nakano (1984).

The dependence of v_{Bx} on B changes considerably with the density. This change is related to the interchange of the dominant process of field dissipation. Fig. 2 shows the ratio D of the effects of plasma drift and Joule dissipation defined by equation (48) for the same model as in Fig. 1. The critical field B_{cr} and the states of $|\tau_{\nu}\omega_{\nu}|=1$ are also shown by the dot-dashed and the dashed lines, respectively. Fig. 3 shows the relative abundances $n(\mathrm{X})/n_{\mathrm{H}}$ of the major types X of charged particle for the model of Figs 1 and 2. The electrical conductivity σ_{c} given by equation (41) is also shown by the dashed curve. The temperature T and the ionization rate $\zeta(\chi)$ given by equation

(54) are shown in the upper part of the figure by the dashed and the dot-dashed curves, respectively.

At a density $n_H<10^{11}\,cm^{-3}$ where ions and electrons are the main charged particles, the plasma drift is dominant when $|\tau_e\omega_e\tau_i\omega_i|>1$ as shown in Section 2.2. In such a situation we have from equations (23), (29) and (37) that

$$v_{Bx}\simeq\frac{\tau_i}{\varrho_i}\frac{1}{c}(\mathbf{j}\times\mathbf{B})_x\simeq\frac{\tau_i}{\varrho_i}\frac{B^2}{4\pi R}. \tag{58}$$

Thus v_{Bx}/u_f is proportional to B^2.

Around $n_H\simeq10^{11}\,cm^{-3}$ the curve of $D=1$ behaves in a complicated way. When $n_+\simeq n_-\gg(\tau_i\omega_i/\tau_+\omega_+)n_i\simeq10^4 n_i$ as is satisfied at $n_H\gg10^{12}\,cm^{-3}$, the plasma drift is dominant only when $|\tau_+\omega_+\tau_-\omega_-|>1$. This condition is not satisfied even with the critical field B_{cr}. Thus, Joule dissipation is dominant at $n_H\gtrsim10^{11}\,cm^{-3}$. When $D\ll1$, i.e. $|\tau_\nu\omega_\nu|\ll1$ for main charged particles, we have from equations (23), (29), (37) and (41) that

$$v_{Bx}\simeq\frac{c^2}{B^2\sigma_c}\frac{1}{c}(\mathbf{j}\times\mathbf{B})_x\simeq\frac{c^2}{4\pi\sigma_c R}. \tag{59}$$

Thus the ratio v_{Bx}/u_f is independent of B as long as the field configuration is such that $(1/c)(\mathbf{j}\times\mathbf{B})_x\simeq B^2/4\pi R$. The time-scale $R/v_{Bx}\simeq4\pi\sigma_c R^2/c^2$ obtained from equation (59) is just the usual time-scale of Joule dissipation. In such a situation, any weak field cannot be retained in a cloud as long as $(1/c)(\mathbf{j}\times\mathbf{B})_x\simeq B^2/4\pi R$ as has been shown by Nakano (1984). Nearly current-free fields with the curvature radius of field lines much greater than the characteristic length of the cloud can exist even in such a situation. The cloud contracts across the field and becomes effectively non-magnetic in its dynamic properties.

The electrical conductivity $\sigma_c(\nu)$ due to particle ν is proportional to the relative abundance of ν, n_ν/n_H, as seen from equation (42). As shown in Fig. 3, σ_c is nearly proportional to n_e/n_H at $n_H\lesssim10^{12}\,cm^{-3}$. This means that σ_c is mainly contributed by electrons and ions. In such a situation we have from equations (11), (42) and (A1) that

$$\frac{\sigma_c(i)}{\sigma_c(e)}=\frac{\mu_{en}\langle\sigma v\rangle_{en}}{\mu_{in}\langle\sigma v\rangle_{in}}\frac{n_i}{n_e}\simeq2\left(\frac{m_e}{m_n}\right)^{1/2}\frac{n_i}{n_e}. \tag{60}$$

Thus $\sigma_c(e)$ is about 30 times greater than $\sigma_c(i)$ at $n_H\lesssim10^{10}\,cm^{-3}$ where $n_i\simeq n_e$. Since n_i/n_e approaches the limiting value $(S_e m_i/m_e)^{1/2}$ at $n_H\gtrsim10^{11}\,cm^{-3}$ where S_e is the sticking probability of electrons on grains (Umebayashi 1983; Nakano 1984), equation (60) becomes

$$\frac{\sigma_c(i)}{\sigma_c(e)}\simeq2\left(S_e\frac{m_i}{m_n}\right)^{1/2}. \tag{61}$$

Because $S_e\simeq1$ at $T\lesssim10^2\,K$ (Umebayashi & Nakano 1980), $\sigma_c(i)$ dominates $\sigma_c(e)$ at $n_H\gtrsim10^{11}\,cm^{-3}$. Because S_e decreases considerably at high temperatures (Umebayashi 1983), $\sigma_c(i)/\sigma_c(e)$ decreases as T increases. At $n_H\gtrsim10^{12}\,cm^{-3}$ the density of ions is at least 10^4 times smaller than that of charged grains. Then $\sigma_c(+)$ and $\sigma_c(-)$ become dominant, and σ_c decreases slowly in proportion to n_+/n_H as seen from Fig. 3.

The ratios v_{Bx}/u_f for spherical clouds of mass $M=10^2$ and $10^{-2}\,M_\odot$ are shown in Figs 4 and 5, respectively. For $M=10^{-2}\,M_\odot$ we have omitted the density region $n_H<10^9\,cm^{-3}$ because the contraction of the cloud is inhibited by the gas pressure at such densities. The results for these two clouds are essentially the same as in Fig. 1. The dissipation of magnetic fields is inefficient at $n_H\ll10^{11}\,cm^{-3}$. Around $n_H\simeq10^{11}\,cm^{-3}$ the magnetic field begins to decouple from the gas; at

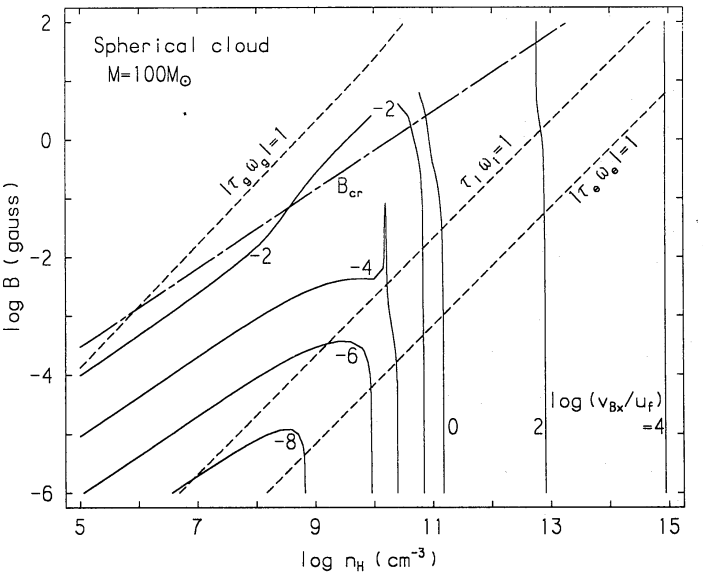

Figure 4. The drift velocity v_{Bx} of the magnetic field as a function of the mean density $n_{\rm H}$ and the mean field strength B for a spherical cloud of $10^2\,M_\odot$. The curves have the same meanings as in Fig. 1.

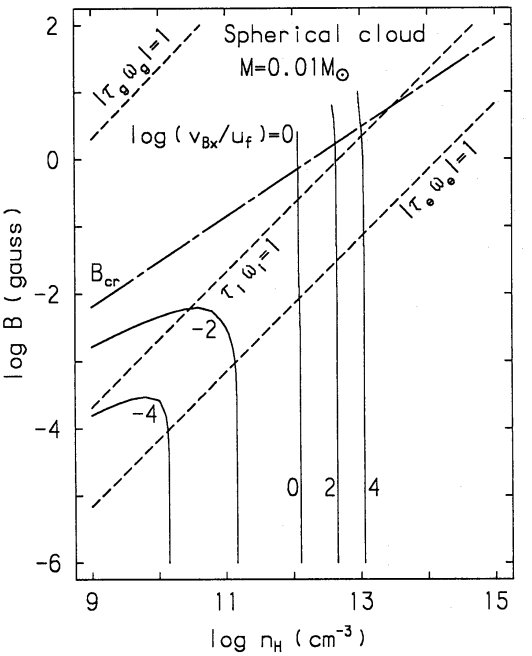

Figure 5. The drift velocity v_{Bx} of the magnetic field as a function of the mean density $n_{\rm H}$ and the mean field strength B for a spherical cloud of $10^{-2}\,M_\odot$. The curves have the same meanings as in Fig. 1.

$n_{\rm H}\gtrsim 10^{12}\,{\rm cm}^{-3}$, at least the curvature of the field lines decreases greatly because of Joule dissipation and only nearly current-free fields can exist.

For a cloud of $M\lesssim 10^2\,M_\odot$ the critical density at which $v_{Bx}/u_{\rm f}\simeq 1$ holds is closely related to the density at which charged grains become the overwhelming majority among charged particles. Since the attenuation of cosmic rays is significant around such densities especially in massive clouds, the critical density decreases slowly as M increases.

When the magnetic field is strong, the cloud deviates considerably from a sphere. Therefore, we shall next consider a flat cloud as another limiting case. Since the cloud can contract faster

along the magnetic field than across the field, the cloud may have attained quasi-equilibrium in which the pressure force along the field nearly balances the gravity. Then the characteristic length of the cloud along the field is approximately given by

$$Z \simeq \left(\frac{k_B T}{4\pi G \mu m_H \varrho} \right)^{1/2}, \tag{62}$$

where k_B is the Boltzmann constant. If the mean density ϱ is set equal to a half of the central density of the cloud, Z is equal to the scale height of an isothermal disc. Since the temperature changes moderately inside the cloud, we can take $s=4\varrho Z$ which holds for an isothermal disc. Thus s and Z are determined as functions of ϱ and T irrespective of the cloud mass M. The semimajor axis R is determined by equation (53) as a function of ϱ, T and M. The mean value of $(1/c)(\mathbf{j}\times\mathbf{B})_x$ in equation (37) now has the form $B^2/4\pi Z$.

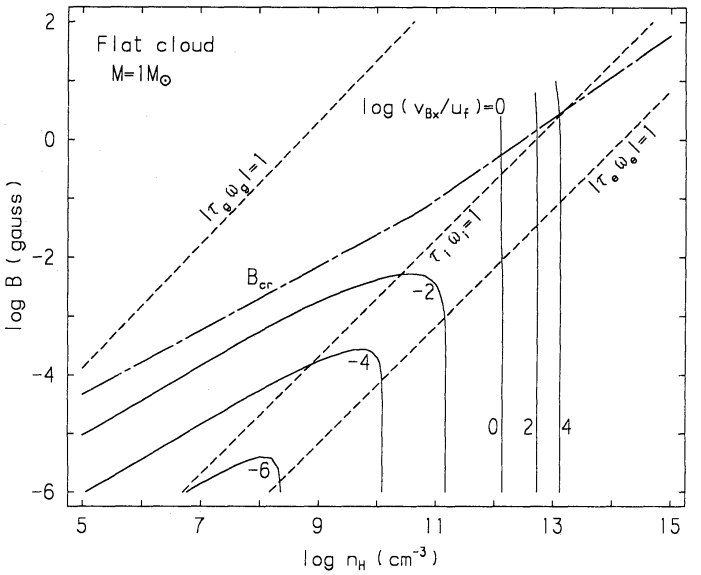

Figure 6. The drift velocity v_{Bx} of the magnetic field as a function of the mean density n_H and the mean field strength B for a flat cloud of 1 $M_\odot$. The solid curves represent the contours of constant v_{Bx}/u_f, u_f being the free-fall velocity. The other curves have the same meanings as in Fig. 1.

Fig. 6 shows v_{Bx}/u_f for a flat cloud of $M=1\,M_\odot$. The critical field strength B_{cr} and the states of $|\tau_\nu\omega_\nu|=1$ are also shown by the dot-dashed and dashed curves, respectively. The curve of B_{cr} is not a straight line because s depends on T as well as on n_H in this case. In Fig. 6 the free-fall velocity u_f is the only quantity which depends on M. Because u_f is proportional to $M^{1/4}$ for a given n_H, we can easily estimate v_{Bx}/u_f for other cloud masses.

The results for such flat clouds are qualitatively similar to those for spherical clouds. At $n_H \lesssim 10^{10}\,\mathrm{cm}^{-3}$, v_{Bx}/u_f is smaller than about 0.1 as long as $B \lesssim B_{cr}$. This is consistent with the results of Nakano & Umebayashi (1980) and of Nakano (1981, 1984). Around $n_H \simeq 1\times10^{12}\,\mathrm{cm}^{-3}$ the drift velocity v_{Bx} exceeds u_f, and the magnetic field decouples from the gas above this density. Since Joule dissipation is dominant, the critical density at which $v_{Bx}/u_f=1$ holds is nearly independent of the field strength. Such a behaviour of the cloud around $n_H \simeq 10^{12}\,\mathrm{cm}^{-3}$ agrees with Nakano's (1984) results for a flat cloud. Although the column density of a flat cloud is much smaller than that of a spherical cloud with $M \gtrsim 1\,M_\odot$ for a given density n_H, the critical density for $v_{Bx}/u_f=1$ is only slightly higher for flat clouds.

3.2 SPATIAL DISTRIBUTION OF v_{Bx}

We have found in Section 3.1 that the magnetic field in clouds of stellar mass decouples from the gas when the mean hydrogen density $\bar{n}_{\rm H}$ is of the order of $10^{12}\,{\rm cm}^{-3}$. However, both the quasi-static and the dynamic contractions of clouds are highly non-homologous. Therefore, it is necessary to investigate the spatial distribution of the drift velocity v_{Bx} in the cloud.

Since the results obtained in Section 3.1 are not sensitive to the shape of clouds, we consider spherical clouds as a limiting case. We investigate the following two cases on the density distribution: (a) a relatively uniform distribution represented by the Emden solution of polytropic index $N=1.5$; (b) a centrally condensed distribution represented by that of $N=4.0$.

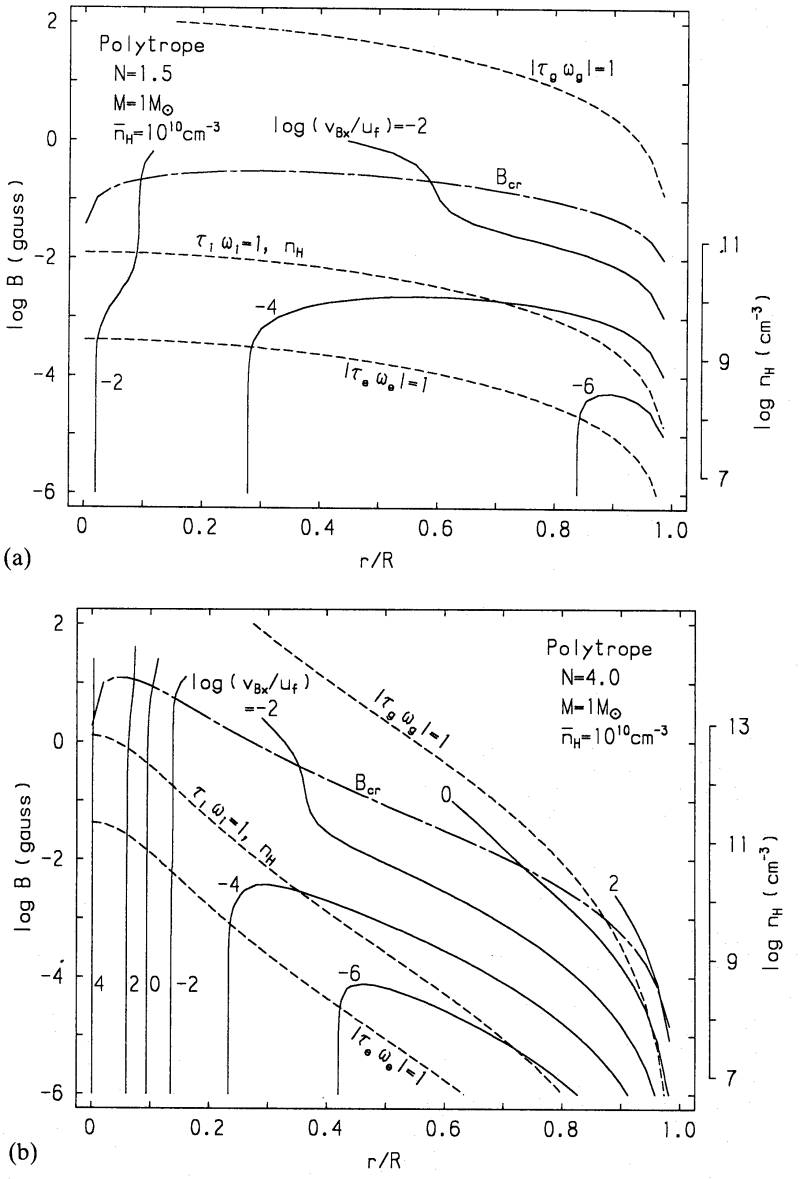

Figure 7. The drift velocity v_{Bx} of the magnetic field as a function of radius r and field strength B for a spherical cloud of mass $M=1\,M_\odot$ and mean density $\bar{n}_{\rm H}=10^{10}\,{\rm cm}^{-3}$ with a density distribution of polytropic index (a) $N=1.5$ and (b) $N=4.0$. The abscissa r is normalized to the cloud radius $R=2.7\times10^{15}$ cm. The solid curves represent the contours of constant $v_{Bx}/u_{\rm f}$ and are labelled by the values of $\log(v_{Bx}/u_{\rm f})$. The critical field $B_{\rm cr}$ for contraction given by equation (63) is shown by the dot-dashed curve. The dashed curves represent the field strength for the state $|\tau_\nu\omega_\nu|=1$ for electrons, ions and grains of charge $\pm e$. The density distribution $n_{\rm H}$ is also shown by the dashed curve for ions with the scale on the right-hand side.

The drift velocity v_{Bx} is insensitive to the temperature unless it is higher than several hundred kelvins. The ionization rate at a spherical shell of radius r is given by equation (54), where χ in this case is the depth of the shell from the cloud surface of radius R. The drift velocity v_{Bx} is calculated by substituting $B^2/4\pi R$ for $(1/c)(\mathbf{J}\times\mathbf{B})_x$ in equation (37). We restrict ourselves to the field strength B smaller than the critical field $B_{\rm cr}$ for contraction given by

$$\frac{B_{\rm cr}^2}{4\pi R}\simeq\varrho(r)\,\frac{GM(r)}{r^2}, \tag{63}$$

where $\varrho(r)$ is the density at radius r and $M(r)$ is the mass contained inside the sphere of radius r. We compare v_{Bx} with the free-fall velocity at r,

$$u_{\rm f}=\left[\frac{2GM(r)}{r}\right]^{1/2}. \tag{64}$$

The results for a cloud of $M=1\,M_\odot$ with a mean hydrogen density $\bar{n}_{\rm H}=10^{10}\,{\rm cm}^{-3}$ (the cloud radius $R=2.7\times10^{15}\,{\rm cm}$) are shown in Fig. 7(a) and (b) for density distributions of $N=1.5$ and $N=4.0$, respectively. The cloud is assumed isothermal with $T=10\,{\rm K}$. Contours of constant $v_{Bx}/u_{\rm f}$ are shown by the solid curves. The critical field $B_{\rm cr}$ for contraction, given by equation (63) is shown by the dot-dashed curve, and the field strengths for the state $|\tau_\nu\omega_\nu|=1$ given by equation (57) are shown by the dashed curves. The density distribution $n_{\rm H}$ is also shown by the dashed curve with the scale on the right-hand side.

The dissipation of magnetic fields is inefficient in the cloud of $N=1.5$. In the cloud of $N=4.0$, however, we find that $v_{Bx}/u_{\rm f}>1$ and then the magnetic field is decoupled from the gas in a small core of $r/R\simeq0.1$. The density $n_{\rm H}$ in this core is higher than $1.8\times10^{12}\,{\rm cm}^{-3}$, and Joule dissipation is predominant. The mass of this core is about $0.30\,M_\odot$. As shown in Fig. 7(b), v_{Bx} exceeds $u_{\rm f}$ in the outermost region of the cloud. At $r/R=0.9$, for example, we find that $n_{\rm H}=2.0\times10^5\,{\rm cm}^{-3}$ while the mean interior density is $1.4\times10^{10}\,{\rm cm}^{-3}$. Thus a diffuse envelope is imposed with very strong gravity and magnetic force. This is why $v_{Bx}/u_{\rm f}$ is large in this region.

The results for a cloud of $M=1\,M_\odot$, $\bar{n}_{\rm H}=10^{12}\,{\rm cm}^{-3}$ (the cloud radius $R=5.9\times10^{14}\,{\rm cm}$) and $N=1.5$ are shown in Fig. 8. We have adopted the temperature distribution

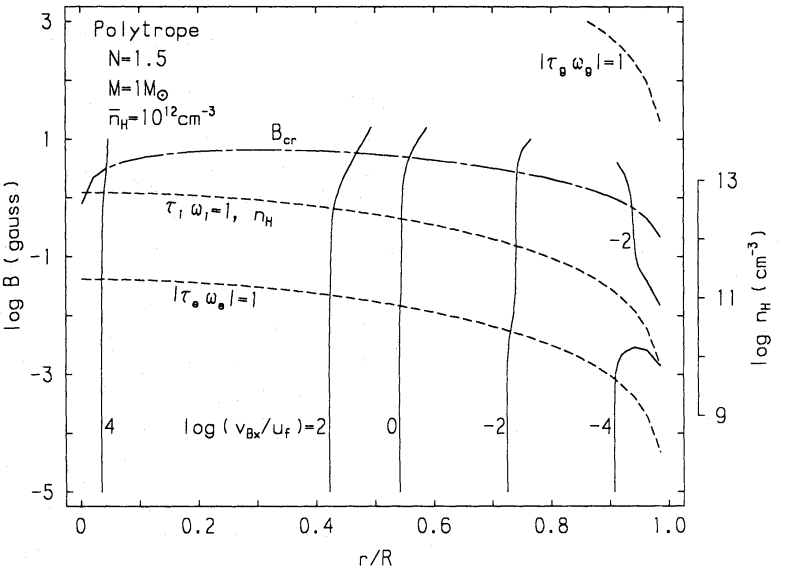

Figure 8. The drift velocity v_{Bx} of the magnetic field as a function of radius r and field strength B for a spherical cloud of $M=1\,M_\odot$ and mean density $\bar{n}_{\rm H}=10^{12}\,{\rm cm}^{-3}$ with the density distribution of polytropic index $N=1.5$. The curves have the same meanings as in Fig. 7.

$T=\min\{100(\varrho/\varrho_c)^{0.2}, 10\}$ in kelvins, where ϱ and ϱ_c are local and central densities, respectively. As mentioned above, the results are not sensitive to T. In the region of $r/R\lesssim 0.54$, v_{Bx} is greater than u_f and then the magnetic field is decoupled from the gas. The density n_H of the region is higher than $2.0\times10^{12}\,\mathrm{cm^{-3}}$, and a mass of about $0.53\,M_\odot$ is contained in this region.

We have also investigated a cloud of $M=1\,M_\odot$, $\bar{n}_H=10^{12}\,\mathrm{cm^{-3}}$ and $N=4.0$ and have found that the magnetic field is decoupled from the gas at $r/R\lesssim 0.3$ where the density is higher than $5\times10^{12}\,\mathrm{cm^{-3}}$. The mass contained in this region is about $0.9\,M_\odot$.

In all these models the magnetic field is decoupled from the gas in the region of $n_H\gtrsim10^{12}\,\mathrm{cm^{-3}}$. This critical density is nearly equal to the critical mean density obtained in Section 3.1.

4 Discussion

We have found in Section 3 that the drift velocity v_{Bx} of magnetic field is much greater than the free-fall velocity u_f at $n_H\gtrsim10^{12}\,\mathrm{cm^{-3}}$ as long as $(1/c)(\mathbf{j}\times\mathbf{B})_x\simeq B^2/4\pi Z$. However, most heavy elements are condensed in grains. Therefore, one may be interested in the drift velocity of grains in such a situation in relation to the chemical composition of newborn stars.

From equations (30) and (37) we have for grains of charge $\pm e$.

$$v_{gx}=\frac{1}{\tau_g^2\Omega_g^2}\left(\tau_g^2\omega_g^2+\frac{A_2}{A_1}\tau_g\omega_g\right)v_{Bx}, \tag{65}$$

where the subscript g is used in place of either + or −. From this equation we find that $|v_{gx}|$ is smaller than v_{Bx} in any situation. Therefore, grains are scarcely lost from the cloud when $v_{Bx}\ll u_f$. At $n_H\gtrsim10^{12}\,\mathrm{cm^{-3}}$ where v_{Bx} may exceed u_f, $|\tau_g\omega_g|$ is much smaller than unity, and we find from the abundances of charged particles and equation (65) that $|v_{gx}|$ is not only much smaller than v_{Bx} but also much smaller than u_f for all models investigated in Section 3. Thus, charged grains move together with the neutrals even when the magnetic field is left behind. In addition, less than 30 per cent of grains are charged at $n_H\gtrsim10^{12}\,\mathrm{cm^{-3}}$. Therefore, no significant fractionation of chemical elements occurs in the processes of star formation.

We shall check some assumptions adopted in this paper.

Epstein's law for the gas drag force on grains is valid only when the motion of grains relative to the gas is subsonic (see Appendix). Because the drift velocity of grains is very small, this condition is always satisfied.

As shown in the Appendix, Langevin's rate coefficients for collisions of ions and electrons with neutrals are valid only when the relative velocity is smaller than the critical velocity $v_c=1.5\times10^6\,\mathrm{cm\,s^{-1}}$ and $5.0\times10^8\,\mathrm{cm\,s^{-1}}$, respectively (although the critical velocities for He are slightly smaller, He is minor both in abundance and in rate coefficient). When $|\tau_\nu\omega_\nu|\gg1$ for ions and electrons, we have from equations (23), (24), (30), (31), (37) and (38) that $v_{\nu x}\simeq v_{Bx}$, $v_{\nu y}\simeq v_{By}$ and $|v_{By}|\lesssim v_{Bx}$. When $|\tau_\nu\omega_\nu|\ll1$, the drift velocity is considerably smaller. For a model of $M=1\,M_\odot$ shown in Figs 1–3, for example, the drift velocity of ions exceeds the critical velocity only at $n_H\gtrsim10^{12}\,\mathrm{cm^{-3}}$ and $B\simeq B_{cr}$. The free-fall velocity u_f in this cloud exceeds this critical velocity only at $n_H\gtrsim10^{14}\,\mathrm{cm^{-3}}$. Therefore, even with a corrected rate coefficient for ions, the drift velocities v_{ix} and v_{Bx} are greater than u_f at $10^{12}\,\mathrm{cm^{-3}}\lesssim n_H\lesssim10^{14}\,\mathrm{cm^{-3}}$ as long as $(1/c)(\mathbf{j}\times\mathbf{B})_x\simeq B^2/4\pi Z$. Because the corrected rate coefficient is proportional to the drift velocity, v_{ix} and v_{Bx} are at least $10^2 u_f$ at $n_H\gtrsim10^{14}\,\mathrm{cm^{-3}}$. Therefore, we need not modify the conclusion obtained in Section 3 that the magnetic field is decoupled from the gas at $n_H\gtrsim10^{12}\,\mathrm{cm^{-3}}$.

We have also made some computations in order to clarify the effects of the parameters regarding the densities of charged particles, and obtained the following results:

(1) The densities of charged particles change only within a factor of 3 for the grain radius a between 3×10^{-6} and 3×10^{-5} cm and the sticking probability S_e of an electron on the grain between 0.01 and 1.0 (Umebayashi 1983). Although the momentum-transfer rate coefficient for a grain $\langle\sigma v\rangle_{gn}$ is proportional to a^2 as shown by equation (A3), v_{Bx} depends weakly on $\langle\sigma v\rangle_{gn}$. Therefore, the basic results obtained in Section 3 are hardly affected by a and S_e.

(2) When T is less than several hundred kelvins and the desorption of charged particles from grains is negligible, the densities of charged particles are insensitive to T (Umebayashi 1983). Other quantities such as $\langle\sigma v\rangle_{gn}$ depend only weakly on T. Therefore, the results obtained in Section 3 are affected little by T. Around several hundred kelvins the desorption begins to dominate over other grain-surface reactions. Electrons and ions become again the major charged particles, and their abundances increase extensively with T. However, around the same temperature the thermal ionization becomes efficient, and it becomes the predominant process of ionization above 10^3 K (Umebayashi 1983). Therefore, the desorption is important only in a narrow range of temperature.

So far we have assumed ionization–recombination equilibrium in determining the densities of charged particles. This assumption holds when the relaxation time of each charged constituent to an equilibrium state is much smaller than the characteristic time-scale of the cloud. When the desorption of charged particles from grain surfaces and the thermal ionization are negligible, the rate equation for constituent X_i is written as

$$\frac{dn(X_i)}{dt}=\sum_j \gamma_{ij}\zeta n(X_j)+\sum_{j,k}\beta_{ijk}n(X_j)n(X_k), \tag{66}$$

where $n(X_i)$ is the number density of X_i, $\gamma_{ij}\zeta$ is the rate of formation of X_i by the ionization of X_j and β_{ijk} is the rate coefficient of collisional reactions such as ion–neutral reactions and ion–electron recombination reactions in the gas phase and the grain-surface reactions. Then the time-scale $t_I(X_i)$ in which X_i approaches the ionization–recombination equilibrium is approximately given by the minimum value of

$$\left|\frac{n(X_i)}{\beta_{ijk}n(X_j)n(X_k)}\right|. \tag{67}$$

We have estimated $t_I(X_i)$ with the equilibrium abundances of constituents shown in Fig. 3. The results are shown in Fig. 9. The viscous damping times for ions and grains, denoted τ_i and τ_g, respectively, and given by equation (11) are shown by dashed lines. The free-fall time $t_f=(3\pi/32G\varrho)^{1/2}$ is also shown by the dot-dashed line for comparison.

At $n_H\ll10^{12}\,\mathrm{cm}^{-3}$ the relaxation time $t_I(X_i)$ is smaller than t_f for all charged particles. Therefore, the gas is nearly in ionization–recombination equilibrium. At $n_H\gtrsim10^{12}\,\mathrm{cm}^{-3}$, however, the relaxation time for grains is greater than t_f. At these densities the grains of charge $\pm e$ are the main charged particles, and the recombination occurs mainly through grain–grain collisions (Umebayashi 1983). As shown in Fig. 3, the 'ionization degree' n_+/n_H in equilibrium decreases with n_H. Therefore, the ionization degree in a contracting cloud is higher than that in equilibrium. If grain–grain collisions are negligible, n_+/n_H is constant (Umebayashi 1983; Nakano 1984). Nakano (1984) investigated the dissipation of magnetic fields by neglecting grain–grain collisions and found that the magnetic field decouples from the gas at $n_H\gtrsim10^{12}\,\mathrm{cm}^{-3}$. Thus the deviation from ionization–recombination equilibrium at such high densities has no important effects on the behaviour of magnetic fields.

In equations (3) and (4) we neglected the effects of momentum transfer between constituents accompanying the transitions of charge states of particles. As shown in Fig. 9, the transition times

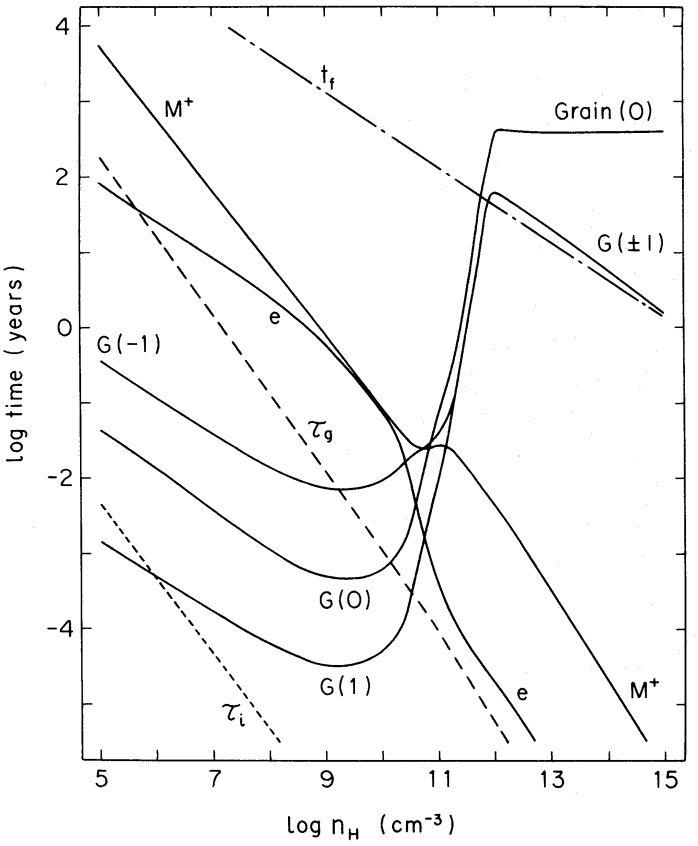

Figure 9. The time-scales of attaining the ionization–recombination equilibrium for some types of charged particle as functions of the density n_H (solid curves) for a spherical cloud of $M=1\,M_\odot$ shown in Figs 1–3. The dashed lines show the viscous damping times of motion relative to neutrals τ_ν for ions and grains given by equation (11). For comparison the free-fall time $t_f=(3\pi/32G\rho)^{1/2}$ is shown by a dot-dashed line.

t_I of ions and electrons are much greater than τ_i and τ_e, respectively ($\tau_e\simeq 6\times10^{-4}\,\tau_i$). Therefore, these effects are negligible compared with those due to frictional forces.

Because the charge of a grain changes stochastically by the sticking of ions and electrons, the grain in a magnetic field moves in a complicated way (Elmegreen 1979). As shown in Fig. 9, the time-scales of charge change of grains are much smaller than τ_g at $n_H\lesssim10^9\,cm^{-3}$. In addition, $|\tau_g\omega_g|\lesssim1$ at $n_H\gtrsim10^5\,cm^{-3}$ and $B\lesssim B_{cr}$. Thus the charge of grains changes in a time-scale much shorter than the time-scales of their motion. Therefore, their motion is approximated by the motion of a grain with a mean charge. This conclusion has also been reached by Nakano & Umebayashi (1980).

In Section 2 we have assumed $d\mathbf{u}_\nu/dt\simeq d\mathbf{u}_n/dt$ for all charged particles. As shown in Fig. 9, all the viscous damping times τ_ν are much smaller than t_f. Therefore, $d\mathbf{u}_\nu/dt$ does not deviate much from $d\mathbf{u}_n/dt$.

Recently, Norman & Heyvaerts (1985) investigated the dissipation of magnetic fields in clouds of density n_H up to $10^{13}\,cm^{-3}$ taking account of only electrons and ions as the charged particles. Introducing an anomalous electrical resistivity caused by the current-driven instabilities which are known in laboratory plasmas, they concluded that the magnetic field dissipates at a density n_H between 10^{11} and $10^{12}\,cm^{-3}$. Although the process proposed by them is quite different from the processes investigated in this paper, it is interesting that both give a similar critical density at which the magnetic field decouples from the gas.

We have shown that substantial flux leakage will occur at $n_H\gtrsim10^{12}\,cm^{-3}$ if the temperature is

low enough. However, the temperature rises with contraction at these densities and this problem will be discussed further in Paper II.

Acknowledgments

The authors thank Professor C. Hayashi for valuable discussions. Numerical computations were carried out at the Data Processing Center of Kyoto University. One of the authors (TU) is indebted to the Japan Society for the Promotion of Science for financial aid in fiscal year 1984.

References

Borra, E. F., Landstreet, J. D. & Mestel, L., 1982. *Ann. Rev. Astr. Astrophys.*, **20,** 191.
Cowling, T. G., 1957. *Magnetohydrodynamics*, Interscience, New York.
Elmegreen, B. G., 1979. *Astrophys. J.*, **232,** 729.
Epstein, P. S., 1924. *Phys. Rev.*, **23,** 710.
Field, G. B., 1970. *Mém. Soc. R. Sci. Liège,* **59,** 29.
Hattori, T., Nakano, T. & Hayashi, C., 1969. *Progr. Theor. Phys.*, **42,** 781.
Mestel, L., 1965. *Q. Jl. R. astr. Soc.*, **6,** 265.
Mestel, L., 1966. *Mon. Not. R. astr. Soc.*, **133,** 265.
Mestel, L. & Spitzer, L., Jr., 1956. *Mon. Not. R. astr. Soc.*, **116,** 503.
Nakano, T., 1979. *Publs astr. Soc. Jap.*, **31,** 697.
Nakano, T., 1981. *Progr. Theor. Phys. Suppl.*, No. 70, 54.
Nakano, T., 1982. *Publs astr. Soc. Jap.*, **34,** 337.
Nakano, T., 1983a. *Publs astr. Soc. Jap.*, **35,** 87.
Nakano, T., 1983b. *Publs astr. Soc. Jap.*, **35,** 209.
Nakano, T., 1984. *Fund. Cosmic Phys.*, **9,** 139.
Nakano, T., 1985. *Publs astr. Soc. Jap.*, **37,** 69.
Nakano, T., Ohyama, N. & Hayashi, C., 1968. *Progr. Theor. Phys.*, **39,** 1448.
Nakano, T. & Umebayashi, T., 1980. *Publs astr. Soc. Jap.*, **32,** 613.
Norman, C. & Heyvaerts, J., 1985. *Astr. Astrophys.*, **147,** 247.
Osterbrock, D. E., 1961. *Astrophys. J.*, **134,** 270.
Spitzer, L., Jr., 1963. *Origin of the Solar System,* p. 39, eds Jastrow, R. & Cameron, A. G. W., Academic Press, New York.
Strittmatter, P. A., 1966. *Mon. Not. R. astr. Soc.*, **132,** 359.
Sweet, P. A., 1950. *Mon. Not. R. astr. Soc.*, **110,** 69.
Umebayashi, T., 1983. *Progr. Theor. Phys.*, **69,** 480.
Umebayashi, T. & Nakano, T., 1980. *Publs astr. Soc. Jap.*, **32,** 405.
Umebayashi, T. & Nakano, T., 1981. *Publs astr. Soc. Jap.*, **33,** 617.
Vogt, E. & Wannier, G. H., 1954. *Phys. Rev.*, **95,** 1190.

Appendix: Momentum-transfer rate coefficients for charged particles in collision with neutral gas particles

We summarize the values of momentum-transfer rate coefficients used in the text and clarify the limits of their applicability in the interstellar clouds.

Electrons and ions are scattered by neutral gas particles mainly through the polarization force. The cross-section for this process has been worked out in detail both classically and quantum mechanically. The momentum-transfer cross-section for an electron or a singly charged ion is classically given by

$$\sigma=\int (1-\cos\theta)\, d\sigma=2.41\pi\left(\frac{e^2\alpha}{\mu v^2}\right)^{1/2}, \tag{A1}$$

where θ is the angle of scattering, α is the polarizability of the neutral particle, and μ and v are the

Table A1. Momentum-transfer rate coefficients $\langle\sigma v\rangle$ ($\mathrm{cm^3\,s^{-1}}$) and critical velocities v_{cr} ($\mathrm{cm\,s^{-1}}$) for the collisions of an electron and a singly charged heavy ion with neutral gas particles.

Neutral particle	Polarizability $\alpha(\mathrm{cm^3})$	Electron $\langle\sigma v\rangle$	v_{cr}	Ion $\langle\sigma v\rangle$	v_{cr}
H_2	8.08×10^{-25}	2.2×10^{-7}	5.0×10^{8}	1.8×10^{-9}	1.5×10^{6}
He	2.05×10^{-25}	1.1×10^{-7}	2.0×10^{8}	6.8×10^{-10}	4.7×10^{5}
Interstellar*	–	2.0×10^{-7}	–	1.6×10^{-9}	–

*Rate coefficients averaged over the chemical composition of $X=0.73$ and $Y=0.25$, the mass fractions of hydrogen and helium.

reduced mass and the relative velocity, respectively (Osterbrock 1961). Here the effect of the strong repulsive force at close distances is approximately taken into account. The quantum correction to the classical cross-section is important only when the dimensionless de Broglie wavevector

$$k=\left(\frac{e^2\alpha\mu}{\hbar^2}\right)^{1/2}\frac{\mu v}{\hbar}, \tag{A2}$$

is much smaller than unity (Vogt & Wannier 1954). The quantum corrections for ions are negligible even for the temperatures in dense clouds and for the polarizabilities of H_2 and He. However, the quantum correction for electrons is not always negligible because of their small mass. Vogt & Wannier (1954) investigated quantum mechanically the cross-section of the capture type which is appropriate to the usual momentum-transfer cross-section and found that the quantum-mechanical cross-section is twice the classical one in the limit of low velocities $k\simeq0$. Thus we can adopt the momentum-transfer cross-section for electrons twice as large as equation (A1) at $T\ll10^3\,\mathrm{K}$.

Since the cross-section is inversely proportional to the velocity, the momentum-transfer rate coefficient averaged over the Maxwellian velocity distribution $\langle\sigma v\rangle$ is independent of the temperature. Values of the rate coefficients are listed in Table A1.

These so-called Langevin's rate coefficients are not correct for relative velocities greater than some critical values v_{cr} because the cross-sections with the polarization force become smaller than the geometrical cross-sections of the neutral and charged particle system, $\sigma_{\mathrm{geom}}=\pi(r_{\mathrm{n}}+r_{\mathrm{c}})^2$, where r_{n} and r_{c} are the radii of the neutral and charged particles, respectively. The values of v_{cr} are also shown in Table A1 for $r_{\mathrm{H_2}}=1.2$ Å, $r_{\mathrm{He}}=1.3$ Å, $r_{\mathrm{e}}\ll1$ Å and $r_{\mathrm{i}}=0.83$ Å. The value of r_{i} is for a representative ion Mg^+ in dense interstellar clouds (Umebayashi & Nakano 1980). These velocities are much greater than the typical thermal velocities in the clouds.

Next we consider the gas drag force on dust grains. In the density region considered in this paper, the mean free path of neutral gas particles is much greater than the size of grains. The relative velocity between the gas and grains is small compared with the sound velocity of gas particles, as has been confirmed in Section 4. In such a situation the gas drag force on a spherical grain is well approximated by Epstein's law (Epstein 1924), and we find that the momentum-transfer rate coefficient for a grain of radius a is given by

$$\langle\sigma v\rangle_{\mathrm{gn}}=\frac{4\pi}{3}a^2c_m \tag{A3}$$

where $c_m=(8k_{\mathrm{B}}T/\pi m)^{1/2}$ is the thermal velocity of a gas particle of mass m. Because grains in dense clouds have only a few excess electrons or ions (Umebayashi & Nakano 1980; Umebayashi 1983) and their typical radius is of the order of 10^{-5} cm, the electric charge of grains has little effect on the rate coefficient.